# A Combination of POD-based Model Order Reduction and Thermal Submodeling for Miniaturized Thermoelectric Generator

M.Sc. C.D. Yuan[1, 2], M.Sc. G. Sadashivaiah[2], M.Sc. S. Kreß[2], Dr. E.B. Rudnyi[3], Prof. Dr.-Ing. T. Bechtold[1, 2]
[1] Department of Engineering, Jade University of Applied Science
Friedrich-Paffrath Str. 101, 26389, Wilhelmshaven, Germany
[2] Institute for Electronic Appliances and Circuits, University of Rostock
Albert-Einstein Str. 2, 18059, Rostock, Germany
[3] CADFEM GmbH, Marktplatz 2, 85567, Grafing b. Munich, Germany

## Abstract

Electrically active implants for regenerative therapies are gaining importance within an aging population of industrial nations. Major drawback of the battery-powered implants is the replacement of the drained power supply. Recently, thermoelectric generator (TEG), which transforms thermal energy into electrical energy, was developed as a power-support for electrically active implants. In this work, a newly designed TEG is incorporated within three-dimensional realistic human torso model. Pennes bioheat equation, is used to describe the heat transfer mechanism in tissue. Convection, radiation, and evaporation effects at the skin surface are applied as boundary conditions. Model order reduction (MOR) via proper orthogonal decomposition (POD) is applied to this nonlinear thermal human torso model to generate an accurate low-dimensional surrogate. Furthermore, for enabling an efficient design optimization of TEG, thermal submodeling approach is combined with POD-based MOR. This technology enables to decouple the thermal-domain simulation of human tissue model from the coupled-domain simulation of TEG model, while keeping the highest accuracy. In this way, an efficient design optimization of the TEG device is enabled.

## 1 Introduction

Aging population is becoming a main concern, especially in Europe, which leads to a large demand for developing medical implants for regenerative therapies, e.g. regeneration of bone tissue, deep brain stimulations for the treatment of motion disorders, and fixing abnormal heart rates with pacemakers. However, with the currently used power-limited batteries and its risk of chemical side effects, medical engineers are encouraged to develop energy harvesting devices for self-powered electrically active implants.

In last decades, various kinds of energy harvesting technologies have been developed for medical implants [1]. In this work, a thermoelectric generator (TEG) is described, which generates electrical power output from the thermal gradient inside human via Seebeck effect. In the previous research [2], the authors designed a squared-shaped TEG integrated in a cubic human tissue model. The temperature difference in TEG was calculated numerically by solving the Pennes bioheat equation [3]. In [4], a disk-shaped TEG was designed and modeled within a simplified cubic human tissue model. Constant metabolic heat generation was considered as the sole heat source and convection was used as the heat transfer effect at the skin surface. To speed up the simulations of such linear thermal finite element (FE) model, Krylov-subspace based model order reduction (MOR) [5] method was implemented to generate a compact and accurate reduced order model (ROM). Later in [6], the authors accounted for the blood perfusion heat generation (nonlinear input) within the system-level simulations based on ROM of TEG. Recently, the authors in [7] managed to incorporate the TEG within more realistic, but still linearized, human forearm model. A new linearization strategy was introduced to solve the nonlinearity caused by the temperature-dependent blood perfusion effect. Furthermore, a combination of Krylov-subspace based MOR and submodeling techniques was introduced.

In this work, we further incorporate the TEG within a realistic human torso model adapted from [8]. Apart from blood perfusion and convection effects, radiation and evaporation effects at the skin surface are considered. Instead of using conventional Krylov-subspace based MOR method, the proper orthogonal decomposition (POD) based MOR [9] is applied. It is further combined with the thermal submodeling technique for enabling efficient design optimization of TEG.

In Section 2, the details of the TEG and human torso model are presented. In Section 3, the combination of POD-based MOR and submodeling methods are introduced. The efficiency and accuracy of this approach will be observed through the achieved results in Section 4. The conclusion of this work and the outlook for future topics are given in Section 5.

# 2 Case Study

## 2.1 Thermoelectric Generator

The TEG is modelled based on a commercially available device. An array of 16×16 p-type and n-type bismuth telluride thermocouples (0.8×0.8×2.27 $mm^3$) are placed between two ceramic plates (each 24.6×24.6×0.565 $mm^3$) (see **Figure 1**). It is surrounded by a disc-shape Teflon housing (height 3.4 mm). The material properties of each part are shown in **Table 1**.

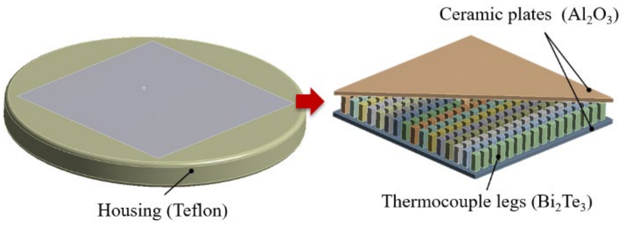


**Figure 1** Assembling setup of the TEG

| TEG parts | Material | Density ($kg/m^3$) | Specific heat (J/kg/K) | Thermal conductivity (W/m/K) |
|---|---|---|---|---|
| Housing | Teflon | 8933 | 385 | 0.25 |
| Plates | $Al_2O_3$ | 3720 | 880 | 25 |
| Thermopile (P-type) | $Bi_2Te_3$ | 7700 | 90 | 1.58~1.52† |
| Thermooile (N-type) | $Bi_2Te_3$ | 7700 | 90 | 1.62~1.58† |

**Table 1** Material properties in TEG
†Varies in temperature between 25°C to 37.5°C

After spatial discretization via FE method, the model contains 127,307 nonlinear ordinary differential equations (ODEs) in total.

## 2.2 Human Torso Model

The realistic human torso model is implemented in ANSYS® Workbench (2019.R1) based on segmented magnetic resonance imaging data from [8] (see **Figure 2**). Realistic human tissue material properties were assigned to various tissue sections. **Table 2** mainly shows the material properties of muscle, fat, skin, and blood tissues. More details and other material properties used, can be found in [10].

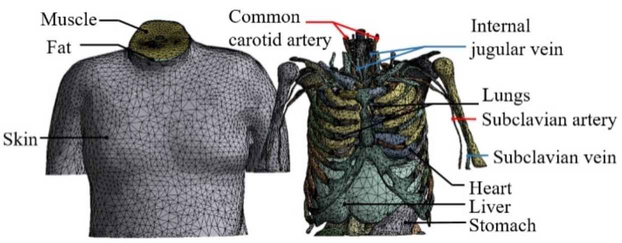


**Figure 2** Torso model contains solid organs, skeleton, main vessels, muscle, fat, and skin layers

As suggested in [2] and [4], the TEG was positioned in the fat layer of left-upper-side chest region (see **Figure 3**), where the maximum temperature gradient was observed.

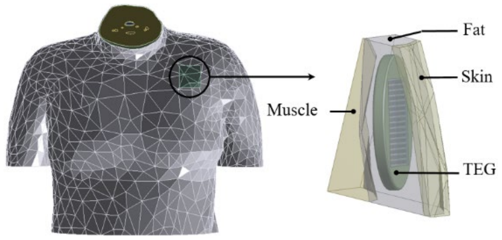


**Figure 3** TEG incorporated within the realistic human tissue model in the chest region

| Tissue | $\rho$ ($kg/m^3$) | $c$ (J/kg/K) | $\omega$ (1/s) | $Q_m$ (W/ $m^3$) |
|---|---|---|---|---|
| Muscle | 1090.4 | 3421.2 | 0.000337 | 498.52 |
| Fat | 911 | 2348.33 | 0.000301 | 279.8 |
| Skin | 1109 | 3390.5 | 0.000906 | 841.57 |
| Blood | 1049.75 | 3617 | / | / |

**Table 2** Muscle, fat, skin and blood tissue properties

The internal heat transfer in human tissue is described by the Pennes bioheat equation:

$$\nabla(\kappa\nabla T) + \underbrace{\rho_b c_b \omega\big(T_a - T(r,t)\big)}_{Q_b} + Q_m = \rho c \frac{\partial T}{\partial t} \quad (1)$$

where $\rho$,c and $\kappa$ are the density, specific heat capacity and thermal conductivity properties of different tissues. T is the unknown temperature state vector and $T_a$ is the arterial blood temperature, which is set as constant at 37°C. $Q_b$ and $Q_m$ are the blood perfusion and metabolic heat generation rates applied in muscle, fat, and skin layers, where $\rho_b, c_b$ describe the thermal properties of blood, and $\omega$ is a measure of perfusion in different tissues. The external heat transfer effects at the skin surface balance the heat generated inside [11]:

$$\begin{aligned} q_{sk} = \underbrace{h_c(T_{skin} - T_{amb})}_{q_{conv}} + \underbrace{\sigma\epsilon\big(T_{skin}^4 - T_{amb}^4\big)}_{q_{rad}} \\ + \underbrace{h_e(P_{skin} - \phi P_{sa})}_{q_{eva}} \end{aligned} \quad (2)$$

where $q_{conv}$, $q_{rad}$, and $q_{eva}$ are the convection, radiation and evaporation heat fluxes normal to the skin surface. $T_{amb}$ is the environmental temperature and $T_{skin}$ is the temperature at the skin surface. The details of the variables in equation (2) are given in [12]. After spatial discretization, the model contains 1,045,949 degrees of freedom and can be represented by a nonlinear-input ODE system as follows:

$$\Sigma_N \begin{cases} E \cdot \dot{T}(t) + A \cdot T(t) = \underbrace{B \cdot u(T(t))}_{F(T(t))} \\ y(t) = C \cdot T(t) \end{cases} \quad (3)$$

where $E, A \in R^{N\times N}$ are the global heat capacity and heat conductivity matrix. $F(T(t))$ captures the nonlinearity of the system. $C \in R^{q\times N}$ is the user defined output matrix with q outputs and $y(t) \in R^q$ is the output vector.

# 3 Combination of POD-based MOR and Thermal Submodeling

Due to the large-size of system (3), it is essential to speed up the simulations of thermal human torso model. Different from the method used in [7], which performs Krylov-subspace based MOR on a linearized thermal human torso model, in this work, the POD-based MOR algorithm was applied to generate a compact but highly accurate surrogate of nonlinear-input system (3). Instead of using orthonormalized Krylov-subspace, another reduced basis (RB) is used as follows:

$$\mathrm{T(t)} \approx \phi_{\mathrm{pod}} \cdot \mathrm{z(t)} \tag{4}$$

where $\mathrm{z(t)} \in \mathrm{R^r}$, $\mathrm{r} \ll \mathrm{N}$, is the reduced state vector and $\phi_{\mathrm{pod}}$ is the RB obtained through POD method. Based on the simulation results of the full-scale model, a snapshot matrix $\mathrm{S} \in \mathrm{R^{N\times n}}$ is constructed by compiling the sampled solution at n time steps:

$$\mathrm{S} = [\mathrm{T(t_1)}, \mathrm{T(t_2)}, \cdots, \mathrm{T(t_n)}] \tag{5}$$

where $\mathrm{T(t_n)} \in \mathrm{R^N}$ represents the temperature distribution results at specific nth time step. To compute the optimal RB $\phi_{\mathrm{pod}}$, a singular value decomposition (SVD) is performed on that snapshot matrix S:

$$\mathrm{S} = \mathrm{U\Sigma V^T} \tag{6}$$

where the columns in $\mathrm{U} = [\phi_1, \phi_2, \cdots, \phi_N] \in \mathrm{R^{N\times N}}$ and $\mathrm{V} = [\xi_1, \xi_2, \cdots, \xi_n] \in \mathrm{R^{n\times n}}$ are left-singular and right-singular vectors of S, respectively. Non-equal vectors $\phi_i, i \in [1, N]$ in U are mutually orthonormal. $\Sigma \in \mathrm{R^{N\times n}}$ is a rectangular diagonal matrix with non-negative singular values $\sigma_i, i \in [1, n]$, which are sorted in descending order at diagonal as $\sigma_1 \geq \sigma_2 \geq \cdots \geq \sigma_n$. The first r leading singular vectors in U are truncated for constructing the optimal RB space:

$$\phi_{\mathrm{pod}} = \mathrm{span}\{\phi_1, \phi_2, \cdots, \phi_r\} \in \mathrm{R^{N\times r}} \tag{7}$$

where the choice of the dimension r is decided by evaluating the relative importance of POD modes through the relative energy equation:

$$\mathrm{E_i} = \frac{\sigma_i^2}{\sum_{i=1}^{n} \sigma_i^2}, i\epsilon[1, n] \tag{8}$$

The sum of the energy in n modes is unity. Usually, the first r modes in U captures 99% of the total energy and preserves the main dynamics of the original system. In conjunction with the Galerkin projection, the full-scale system (3) is projected onto the RB:

$$\Sigma_r \begin{cases} \mathrm{E_r} \cdot \dot{\mathrm{z}}(\mathrm{t}) + \mathrm{A_r} \cdot \mathrm{z(t)} = \mathrm{N(z(t))} \\ \mathrm{y(t)} = \mathrm{C_r} \cdot \mathrm{z(t)} \end{cases} \tag{9}$$

where $\mathrm{E_r} = \phi_{\mathrm{pod}}^{\mathrm{T}} \mathrm{E} \phi_{\mathrm{pod}}$, $\mathrm{A_r} = \phi_{\mathrm{pod}}^{\mathrm{T}} \mathrm{A} \phi_{\mathrm{pod}}$, $\mathrm{C_r} = \mathrm{C}\phi_{\mathrm{pod}}$ are the reduced matrices. The nonlinear-input is reduced as $\mathrm{N(z(t))} = \phi_{\mathrm{pod}}^{\mathrm{T}} \mathrm{F}(\phi_{\mathrm{pod}} \mathrm{z(t)})$. Then, the system (9) is discretized in time and solved with forward Euler method.

In addition, for providing an efficient TEG design optimization method, thermal submodeling technique, available in ANSYS® Workbench, is combined with POD-based MOR. Firstly, a representative TEG model, where the structure of thermocouple legs is replaced by a simple block structure, is embedded into the human torso model (see **Figure 4**). The equivalent material properties of the block structure are chosen based on the experimental data from [13]. This model is reduced by POD-based MOR and solved. Its result $\mathrm{T(t)}$ (recovered through equation (4)) is used as the boundary condition for the detailed TEG submodel (see **Figure 5**). In this way, the design alterations of the TEG submodel can be computed efficiently, that is without repeating simulations of the global human torso model.

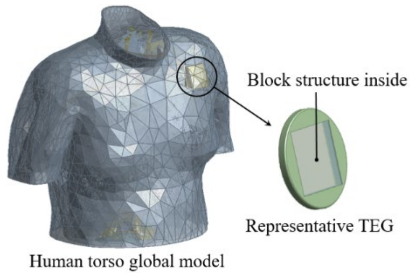


**Figure 4** Human torso model incorporating the representative TEG with block structure

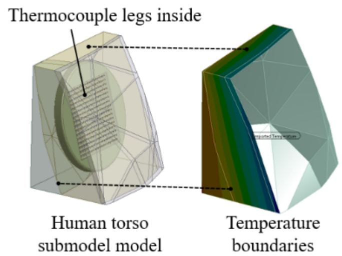


**Figure 5** Human torso incorporating detailed TEG submodel

# 4 Numerical Simulation Results

To obtain the temperature distribution of the model from **Figure 4**, we begin with a steady state simulation with heat transfer coefficient of 3.1 $\mathrm{W/m^2K}$ and ambient temperature of 25 °C. Based on this initial state, a transient simulation is performed with a changed heat transfer coefficient of 5.48 $\mathrm{W/m^2K}$. Then POD-based MOR is applied and temperature results at three selected output nodes in muscle, fat, and skin layers are compared (see **Figure 7**). The maximum relative error between the full and reduced model is 0.035% in the muscle layer. This indicates that the ROM is accurate enough for re-projecting the reduced temperature state vector back to the full size. It can be further used as temperature boundary conditions for the submodel.

Finally, the accuracy of the temperature results obtained through submodeling technique was verified (see **Figure 8**). It was observed that the maximum relative difference between global and submodel simulations was 0.11%.

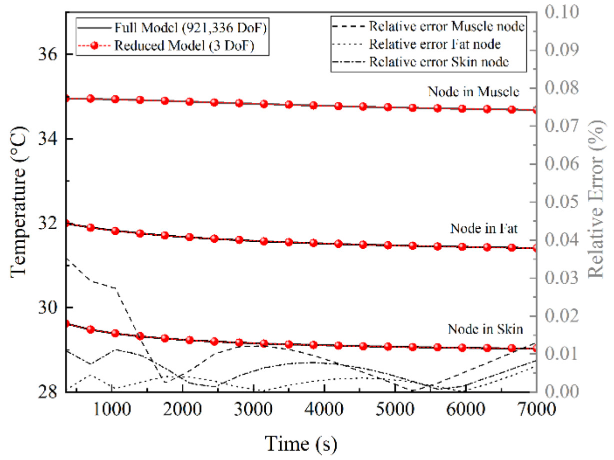


**Figure 7** Temperature results from full (921,336 DoF) vs. reduced (3 DoF) models

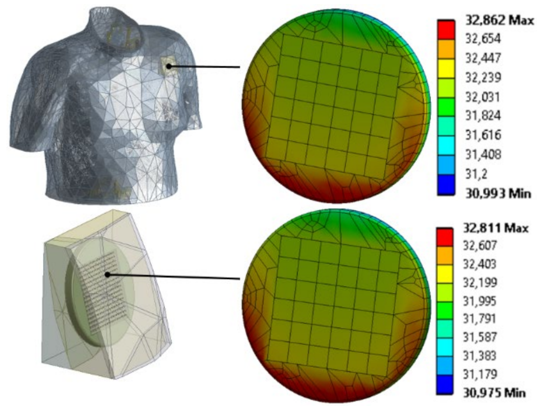


**Figure 8** Comparison of temperature results on detailed TEG via global model and submodel simulations

Through the combination of POD-based MOR and submodeling techniques, the computational time was 6.89 times faster comparing to the full-scale FE simulation (see **Table 3)**. The generation of the snapshot matrix in POD-based MOR was considered as the offline effort.

| Computational time | Detailed TEG as submodel | Detailed TEG in global model |
|---|---|---|
| POD-based MOR | 54.6 s | / |
| Sim. in submodel | 187.73 s | |
| Total | 242.33 s | 1669.56 s |

**Table 3** Computational times comparison
(On HPC with 16× Intel® Xeon® CPU E5-2687W v4 @ 3.00GHz, RAM 324 GB, VGA NVIDIA Tesla M10)

# 5 Conclusion and Outlook

In this paper, we introduced a methodology for efficient design optimization of TEG, which combines POD-based MOR and thermal submodeling techniques. The numerical simulation results shown in Section 4 proved that the accuracy can be preserved within the submodel with much less computational effort.

In the future, parametric model order reduction will be applied to generate parameter-independent reduced order models of TEG. Furthermore, system-level simulation, which incorporates power-management circuitry, will be performed based on the reduced TEG model.

# 6 Literature

[1] A.B. Amar et al., “Power Approaches for Implantable Medical Devices”, In Sensors (Basel), 15(11), 2015, pp. 28889-914.

[2] Y. Yang et al., “Suitability of a Thermoelectric Power Generator for Implantable Medical Electronic Devices”. In Journal of Physics D: Applied Physics, 40(18), 2007, pp. 5790-5800.

[3] H.H. Pennes, “Analysis of tissue and arterial blood temperatures in the resting human forarm”, In Journal of Applied Physiology, 1(2), 1948, pp. 93-122.

[4] O.S. Jadhav et al., “Design of a thermoelectric generator for electrical active implants”, In Mikrosystemtechnik Kongress, 2017, pp. 1-4.

[5] R.W. Freund, “Krylov-subspace methods for reduced order modelling in circuit simulation”, In Journal of Computational and Applied Mathematics, 123(1-2), 2000, pp. 395-421.

[6] O.S. Jadhav et al., “Nonlinear Model Order Reduction of Thermoelectric Generator for Electrically Active Implants”, International Conference on Bioelectromagnetism, 2018.

[7] C.D. Yuan et al., “Efficient Design Optimization of a Thermoelectric Generator by a Combination of Model Order Reduction and Thermal Submodeling Techniques”, Communications of the ECMS, 33(1), 2019, pp. 290-295.

[8] S. Makarov et al., VHP-Female Datasets, NEVA Electromagnetics, LLC, vhp-female 2.2 ed., 2015.

[9] A. Quarteroni et al., “Reduced basis methods for partial differential equations”, Springer Switzerland, 2016, pp. 115-140.

[10] P.A. Hasgall et al., IT’IS Database for thermal and electromagnetic parameters of biological tissues. IT’IS Foundation, Zurich, Switzerland, version 4.0 ed., 2018.

[11] D. Fiala, “Dynamic Simulation of Human Heat Transfer and Thermal Comfort”, Ph. D. Thesis, De Montfort University, 1998.

[12] K. Parsons, “Human thermal environments”, 3rd ed.: CRC Press, Taylor & Francis, 2014.

[13] S.G. Yalkoti, “Characterization of Thermoelectric Energy Conversion for Implantable Medical Devices”. Master Thesis. Department of Computer Science and Electrical Engineering, University of Rostock, Germany, 2017.